A high-resolution life cycle impact assessment model for continental freshwater habitat change due to water consumption

Mattia Damiani, Philippe Roux, Eléonore Loiseau, Nicolas Lamouroux, Hervé Pella, Maxime Morel, Ralph K. Rosenbaum

1 # A high-resolution life cycle impact assessment model for continental

2 # freshwater habitat change due to water consumption

3 *Mattia Damiani*[ac], Philippe Roux [a], Eléonore Loiseau [a], Nicolas Lamouroux [b], Hervé Pella [b],*

4 *Maxime Morel [b], Ralph K. Rosenbaum [a]*

5 [a] ITAP, INRAE, Montpellier SupAgro, Univ Montpellier, ELSA Research Group and ELSA-

6 PACT Industrial Chair, Montpellier, France

7 [b] INRAE Lyon, UR RiverLy, Villeurbanne, France

8 [c] Department of Environmental Sciences, Informatics and Statistics, Ca' Foscari University of

9 Venice, Mestre-Venezia, Italy

10 [*]Corresponding author: damianimtv@gmail.com

11 **ABSTRACT**

12 Global value chains and climate change have a significant impact on water resources and

13 increasingly threaten freshwater ecosystems. Recent methodological proposals for life cycle

14 impact assessment (LCIA), evaluate water use impacts on freshwater habitats based on river

15 hydraulic parameters alterations. However, they are limited to French rivers due to lack of global

16 data and models. On this basis, this article proposes an approach to compute regionalized

17 characterization factors for modeling river habitat change potential (HCP) induced by water

18 consumption, potentially applicable worldwide. A simplified model is developed for fish guilds

19 and invertebrates. Based on French datasets, it establishes a relationship between HCP and river

20 hydraulic parameters. A methodology to derive discharge and hydraulic geometry at the reach

21 scale is proposed and applied to European and Middle Eastern rivers below 60°N latitude.

22 Regionalized HCPs are calculated at the river reach scale and aggregated at watershed. Then, the

impact of agricultural water use in contrasted European and Middle Eastern countries is evaluated comparing the outcomes from the HCP and the Available Water Remaining (AWARE) models at the national scale, considering water supply mix data. The same analysis is carried out on selected river basins. Finally, result consistency, uncertainty and global applicability of the overall approach are discussed. The study demonstrates the reproducibility of the impact model developed for French rivers on any hydrographic network where comparable ecological, hydrological and hydraulic conditions are met. Furthermore, it highlights the need to characterize impacts at a higher spatial resolution in areas where HCP is higher. Large scale quantification of HCP opens the way to the operationalization of mechanistic LCIA models in which the habitat preferences of freshwater species are taken into account to assess the impacts of water consumption on biodiversity.

GRAPHICAL ABSTRACT
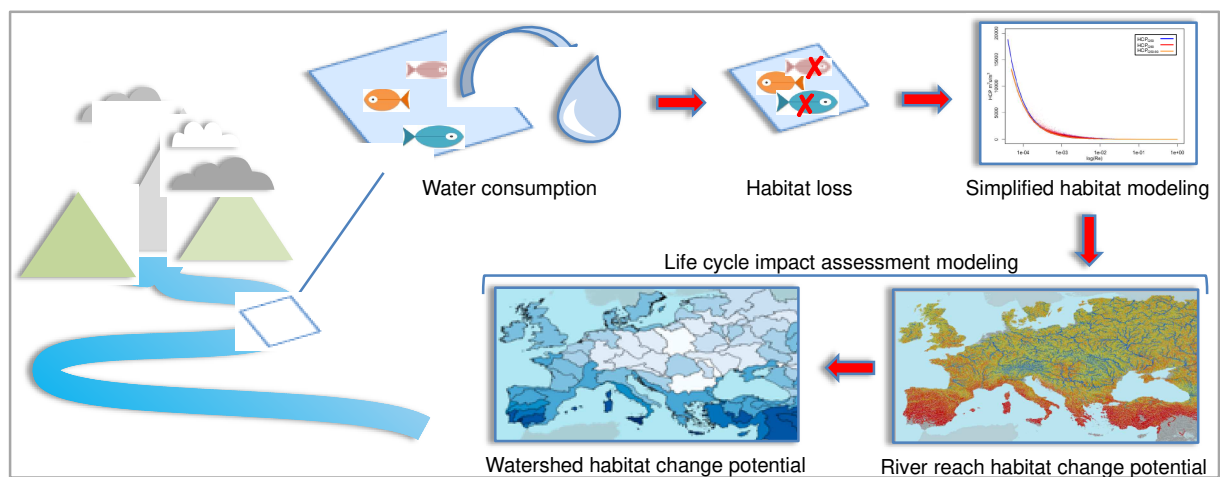
KEYWORDS

Life cycle impact assessment, water consumption, freshwater habitat, biodiversity

38 **ABBREVIATIONS**

39   LCA, life cycle assessment; LCIA, life cycle impact assessment; CF, characterization factor;

40 FF, fate factor; EF, effect factor; HCP, habitat change potential; Q, river discharge; CWU,

41 consumptive water use; HS, habitat suitability; WUA, weighted usable area; Re, Reynolds

42 number; W, river width ; HB, HydroBASINS; WSmix, water supply mix.

1. INTRODUCTION

Human interaction with water systems in the Anthropocene is being expressed through the pervasive alteration of the global water cycle. This stimulated the contextualization of watershed scale management paradigms under a global-scale perspective leading to the production of an increasing amount of knowledge about worldwide freshwater resource availability and exploitation (Vörösmarty et al., 2013). Water use for human activities and the exportation of water-hungry products in globalized supply chains (Dalin et al., 2017; Moran and Kanemoto, 2017), besides the consideration of the geopolitical implications of global water cycle modification, call for a better understanding of effective and potential consequences on water-dependent ecosystems.

More than 50% of the major river basins on Earth are threatened by pollution and disturbance of natural flow regimes, with damming, river fragmentation and consumptive water use among the main causes of biodiversity loss (Vörösmarty et al., 2010). Notwithstanding, estimations of global river threats and biodiversity status are often partial, since small streams are barely captured by global statistics, despite being generally more sensitive to anthropic pressures. High resolution global surface water availability models are nowadays of great importance (Pekel et al., 2016) and the refinement of methods to assess freshwater requirements of ecosystems and biodiversity is needed (Janse et al., 2015; Pastor et al., 2014).

Life cycle assessment (LCA) is a service and product-oriented approach to global-scale analysis of supply chains for various impact categories, including water use. Impact indicators can quantify damage on the environment at the end of a cause-effect chain (i.e. endpoint impact on resources, human health, and ecosystem quality), or describe environmental mechanisms occurring prior to the endpoint (i.e. midpoint). Characterization factors are developed to convert

66 inventory data (e.g. m^3 of water consumed per unit of product) to the corresponding impact

67 indicators. Depending on the type of impact, characterization factors may consider physical

68 change of local environmental conditions caused by a stressor (fate factor), the exposure of

69 sensitive targets (exposure factor), and any related adverse effects (effect factor).

70 AWARE, a consensus model for water use impact assessment in LCA, proposed by the

71 UNEP-SETAC Life Cycle Initiative working group on water use in LCA (WULCA), includes

72 environmental water requirements (EWR) in the quantification of available water remaining for

73 life cycle impact assessment (LCIA) midpoint characterization (Boulay et al., 2018). Pfister et al.

74 (2009) developed endpoint characterization factors for freshwater consumption impacts on net

75 primary productivity (NPP) of vascular plants as a proxy for species loss. The model proposed

76 by Verones et al. (2017, 2013a, 2013b) quantifies potential biodiversity impacts for birds,

77 amphibians, reptiles and mammals in wetlands. Existing LCIA models for riverine species based

78 on species-discharge relationships (Hanafiah et al., 2011; Tendall et al., 2014) have limitations in

79 capturing changes in river communities because they do not consider the different responses that

80 species adapted to different habitats have to river flow reduction or increase (Damiani et al.,

81 2019, 2018). All these models address furthermore the need for regionalized characterization

82 factors, further raised, for instance, with recent LCA application at the territorial scale (Loiseau

83 et al., 2018; Nitschelm et al., 2016), and should ultimately be coupled with spatially explicit

84 information on water supplies (Leão et al., 2018).

85 Modeling at watershed spatial resolution is consistent with widely employed water

86 management practices for river ecosystems protection (Palmer et al., 2009). LCIA should

87 therefore aim at providing global, regionalized models based on mechanistic approaches applied

88 at watershed and sub-watershed levels. At present, no operational mechanistic model to assess

89 water consumption impacts on stream ecosystems is available at the global scale (Damiani et al.,

90 2018; Núñez et al., 2016). A high-resolution midpoint impact indicator of habitat change

91 potential (HCP) based on freshwater physical habitat suitability for fish species, fish guilds and

92 benthic macroinvertebrates has recently been proposed (Damiani et al., 2019). HCP quantifies

93 the potential change in available habitat quantity on a river and watershed scale as a result of

94 water consumption, taking into account the habitat preferences of freshwater fish and

95 invertebrate species. However, the model is only applicable to the French river network and a

96 worldwide extension needs to be investigated. The present study builds on this approach

97 proposing a method for the development of characterization factors for water consumption

98 impacts on freshwater instream ecosystems, to be implemented worldwide.

99 The availability of global data required to apply the habitat suitability equations adopted in the

100 local French mechanistic approach is first evaluated. Based on available databases, missing

101 variables are identified, namely topographical, hydrological and hydraulic. The high-resolution

102 HCP model is then simplified to reduce complexity of input variables and to adapt to their

103 availability. Variables are subsequently calculated from existing models to allow implementation

104 outside France. An application of the new HCP model (referred to as generalized or global HCP

105 throughout the article) on the European continent and the Middle East is then demonstrated and

106 discussed. Characterization factors are calculated at the river reach scale and then aggregated at

107 watershed scale. Results are compared with those of the original local model applied in France

108 and a case study on European agricultural production is presented to show potential similarities

109 and dissimilarities between the generalized HCP model and the AWARE model, since it is the

110 only (proxy-) midpoint method actually including water demand for river ecosystems in the

111 characterization and providing regionalized characterization factors for watersheds worldwide.

2. MATERIALS AND METHODS

2.1 Habitat change potential at river reach scale

Characterization factors based on HCP were computed from Equation 1 (taken from Damiani et al., 2019), where CF_i is the characterization factor at river reach i. FF is the fate factor calculated as the ratio between the difference in river discharge dQ (m^3/s) for each cubic meter of consumptive water use $dCWU$ and it is assumed to be equal to 1 (Hanafiah et al., 2011). EF is the effect factor represented by habitat change potential HCP in $m^2 s/m^3$ (change in m^2 suitable habitat quantity induced by river discharge alteration in m^3/s), then CF = HCP. In Damiani et al. (2019), the authors calculated HCP from seventeen multivariate habitat suitability equations corresponding to four fish guilds with different habitat preferences, eight fish species where some of them at different stage of development (i.e. alevin, juvenile, adult; Lamouroux and Capra, 2002), and a generic equation for benthic macroinvertebrates.

$$CF_i = FF_i \cdot EF_i = \frac{dQ_i}{dCWU_i} \cdot HCP_i \tag{1}$$

HCP values were aggregated at reach scale to facilitate their use in LCIA, resulting in two indicators, one of which gathers guilds and invertebrates HCPs. For a global application of the model, we adopted the latter since we assume it summarizes a sufficiently large spectrum of habitat preferences without referring necessarily to particular species for which the distribution would be uncertain (see Table S1 in Supporting Information – SI – for guilds characteristics). Nevertheless, in the aggregated characterization factor, fish species favoring shallow and running waters dominate the overall characterization factor since their habitat is more sensitive to water quantity alteration.

132   Data availability at the global scale is a major constraint for a worldwide application of the

133   HCP model. In Table 1 input variables of the local HCP model are listed.

134   **Table 1.** Variables required to run the HCP model of Damiani et al. (2019)

Reach Variable	Unit
Upstream catchment area (A)	km^2
Slope (S)	*%*
Strahler order (O)	
Width (calculated from Q, A, S and O)	m
Depth (calculated from Q, A, S and O)	m
Substrate particle diameter	mm
Inter-annual average discharge ($\bar{Q}$)	m^3/s
Inter-annual natural Median daily discharge (*Q50*)	m^3/s
Inter-annual low flow discharge daily percentile (*Q90*), over which daily discharge is 90% of the time	m^3/s

135

136   The model applied in France in Damiani et al. (2019) is based on the French theoretical

137   hydrographical network (RHT, Pella et al., 2012) which has a resolution of the order of meters

138   and provides all input variables needed to quantify habitat change potentials. Data in Table 1

139   with the same spatial precision are currently not available globally. The products derived from

140   the HydroSHEDS database at 15 arc-sec ($\approx$ 500 m at the equator) represent, to our knowledge,

141   the best available option in terms of spatial resolution of river segments and global coverage

142   (Lehner and Grill, 2013), but hydrological, hydraulic and topographical information are seldom

143   associated to such datasets with the same accuracy as in the RHT network.

2.2 Modeling regionalized HCPs worldwide

The difficulty in deriving data at the river reach scale for substrate composition and especially

for flow magnitudes hinders the global parameterization of HCP (e.g. flow exceedance

probability for *Q50* and *Q90* was calculated from daily streamflow data in the RHT network).

For this reason, a generalization of the local HCP model was developed to reduce the data

requirements shown in Table 1. Subsequently, input variables of the simplified model were

calculated for European and Middle Eastern river segments and the results of HCP

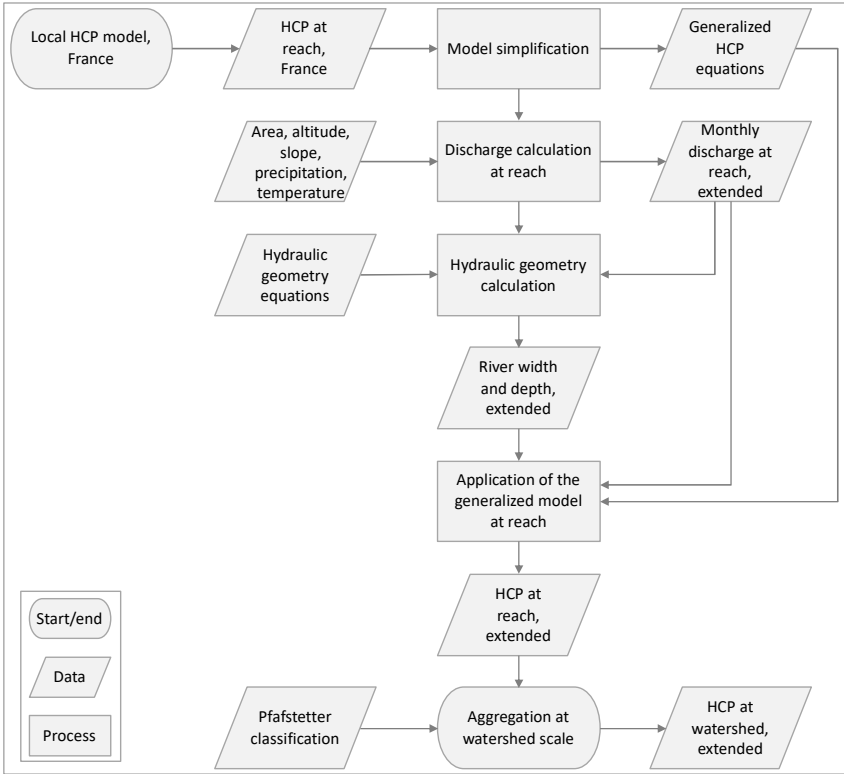characterization at reach were aggregated at watershed scale (Figure 1).

Figure 1. Logical approach for the characterization of habitat change potential at the global

scale, demonstrated on European and Middle Eastern rivers

2.3 Extrapolation of a generalized HCP model

Habitat change potential was quantified on French rivers for *Q50* and *Q90*, representing median and low flows respectively. The discharge-dependent input variable of the LCIA model, which is directly altered by water consumption, is the Reynolds number *Re*, calculated as the ratio between river discharge *Q* and the product of water viscosity *v* (considered equal to 10^{-6} m^2/s) and river width *W*. To avoid working with high values, *Re* is multiplied by 10^{-7} (Damiani et al., 2019; Lamouroux and Capra, 2002; Lamouroux and Souchon, 2002). Non-linear least squares analysis was used to fit a power model to HCP results for *Re* at *Q50* and *Q90* (Equations 2 and 3). Model fitting was carried out in R (R Core Team, 2016; RStudio Team, 2016). When modeling HCP for the world's rivers, defining where and in which period of the year median and low flow conditions occur is not straightforward. To solve this, an equation was derived by fitting the model on *Q50* and *Q90* HCPs together, ranging from -1.8 to 22 396.3 m^2 s/m^3 (Equation 4). The residuals root-mean-squared errors (RMSE) indicate that the average spread of sample data around the regression line is lower than 0.5% of the HCP range for the three equations and can thus provide a measure of the goodness of fit of the simplified models.

$$HCP_{Q50} = 0.439 \cdot \left(\frac{Q50}{v \cdot W50} \right)^{-1.053} \qquad \text{RMSE} = 50 \qquad (2)$$

$$HCP_{Q90} = 0.669 \cdot \left(\frac{Q90}{v \cdot W90} \right)^{-0.998} \qquad \text{RMSE} = 108 \qquad (3)$$

$$HCP_{Q50-90} = 0.614 \cdot \left(\frac{Q}{v \cdot W} \right)^{-1.008} \qquad \text{RMSE} = 86 \qquad (4)$$

In case precise determination of flow exceedance probability is available at the scale of a river segment, Equation 2 and 3 are preferable, otherwise, and for the present study, the HCP_{Q50-90} equation was used to calculate characterization factors in Europe and the Middle East.

173 Nonetheless, as shown in Figure 2, results of the three models are not dissimilar, with HCP$_{Q90}$

174 and HCP$_{Q50-90}$ almost overlapping for high HCP values, and the three curves converging as flow

175 increases.

176
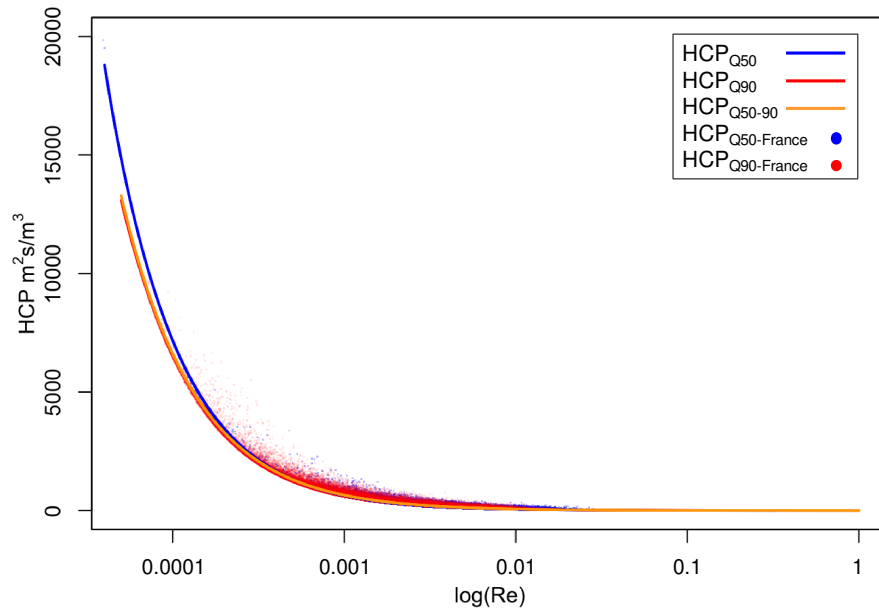
Figure 2. Power models describing HCP variation with Reynolds number. Curves fitted on HCP

values at *Q50* and *Q90* in French rivers

2.4 HCP global model's input variables and application at reach scale

180   As demonstrated by the simplified HCP Equations 2, 3, 4, HCP can be calculated globally

181 from river discharge and width. At present, global flow data estimated at watershed scale are

182 available (WaterGAP, Alcamo et al., 2003; Döll et al., 2003), a global dataset have been recently

183 derived from WaterGAP for discharge at river segment scale (Linke et al., 2019), but yet no *Q50*

184 and *Q90* data are available. A regression model to estimate mean, annual streamflow was

185 recently proposed based on empirical data from globally distributed gauging stations (Equation

186 5, adapted from Barbarossa et al., 2017).

$$Q_{\text{it}} = 10^{9.066} \cdot A_i^{1.018} \cdot H_i^{-0.509} \cdot S_i^{0.464} \cdot P_{\text{it}}^{2.070} \cdot 10^{-0.038 \cdot T_{\text{it}}} \tag{5}$$

187   To improve temporal resolution of existing datasets, in this study, this model was used to

188   calculate discharge at reach i and month t from the input parameters, listed in Table 2 along with

189   the data sources used.

190   **Table 2.** Input data for discharge calculation at river reach (adapted from Barbarossa et al., 2017)

Variable	Unit	Data source	Reference	Resolution	
				Spatial	**Temporal**
Drainage area (A)	m²	A simple global river bankfull width and depth database	Andreadis et al., 2013	15 arc-sec	-
Altitude (H)	m	HydroSHEDS	Lehner and Grill, 2013	15 arc-sec	-
Slope (S)	(°)	HydroSHEDS (calculated)			
Precipitation (P)	m/s	WorldClim	Fick and Hijmans, 2017	30 arc-sec	Month
Temperature (T)	°C	WorldClim			

191

192   Drainage area was taken from the hydraulic geometry dataset of Andreadis et al. (2013) where

193   catchment surface values are associated to each river segment present in the HydroSHEDS 15

194   arc-sec hydrographic network with river segments in desert areas masked out. Minimum,

195   maximum and average altitudes were attributed to each segment based on the HydroSHEDS

196   digital elevation model (DEM) at 15 arc-sec. Reach length was also calculated to be able to

197   derive average slope in degrees according to Equation 5. A factor of 0.5 which is half of the

198   resolution of the DEM, was added to Equation 6 to avoid zero values of slope that would result

199   in zero discharge. It was therefore implicitly assumed that with a slope equal to zero, river reach

200   discharge is fed by upstream water inertial flow.

$$Slope_i = \arcsin\left(\frac{H_{i\,max} - H_{i\,min} + 0.5}{Length_i}\right) \cdot \left(\frac{180}{\pi}\right) \tag{6}$$

201   Precipitation and temperature were derived from the WorldClim database at 30 arc-sec

202   resolution. Considering that the dataset provides climatic data with a monthly resolution,

203   streamflow values (Q) were calculated for each month t, substituting monthly values of P and T

204   in Equation 5. All spatial geoprocessing was carried out using SAGA and QGIS (Conrad et al.,

205   2015; Quantum GIS Development Team, 2017).

206   Currently no global databases are available including width (W) at the reach scale for monthly

207   discharge values. However, hydraulic geometry relationships between discharge, width, depth

208   and velocity have been described extensively and, with some approximation depending on the

209   chosen method, can be computed by models that remain valid worldwide (Leopold and

210   Maddock, 1953; Park, 1977; Rhodes, 1978). In particular, Morel et al. (2020) collected most of

211   the hydraulic geometry data available at the scale of stream reaches. They found high

212   intercontinental similarity in hydraulic geometry models between France and New Zealand,

213   suggesting that their results can be applied globally. Here, to provide global hydraulic geometry

214   relationships that represent variations in width W in space (among reaches) and time (with

215   discharge Q), we used a combination of the "downstream" (in space) and "at-a-station" (in time)

216   formulations of hydraulic geometry of Leopold and Maddock (1953), following the approach of

217   Lamouroux and Souchon (2002) and Morel et al. (2020) (Equation 7):

$$W_{it} = \left[a_d \cdot \bar{Q}_i^{\,b_d}\right] \cdot \left[\frac{Q_{it}}{\bar{Q}_i}\right]^b \tag{7}$$

218   where a_d and b_d are the "downstream" hydraulic geometry parameters for width, and b is the

219   "at-a-station" exponent that describes variations with discharge. We fitted these three parameters

220   to the data from 1304 reaches of France and New Zealand available in Morel et al. (2020), giving

221    $a_d = 7.482$, $b_d = 0.477$, and $b = 0.148$.

222   To demonstrate the applicability of the global HCP model at the reach scale, habitat change

223   potential was quantified on 449 508 river segments covering Europe and the Middle Eastern

224   regions. Since all variables were calculated on rivers derived from SRTM-based datasets

225   (NASA's Shuttle Radar Topography Mission), such as HydroSHEDS, the dataset is limited to

226   rivers below 60°N latitude (taken from Andreadis et al., 2013). The original model developed for

227   French rivers has limited relevance for high flow periods and, in consequence, the derived global

228   model as well. Global HCP was calculated using Equation 4 on a monthly basis because for a

229   large-scale application it is not possible to determine high, median and low flows in regions with

230   different climate and hydrological conditions. For this reason, it is not possible to exclude some

231   months a priori from the characterization. This choice is further discussed in section 4.

232   **2.5 HCP aggregation at watershed scale**

233   Regionalization of characterization factors is necessary because in LCA it is difficult to obtain

234   the detail of local water withdrawal and release, especially for background activities and pre-

235   compiled processes in existing databases, where only average national values are usually

236   available. With regard to the HCP model, the optimal spatial resolution should be a trade-off

237   between habitat model uncertainties at the local scale and HCP spatial variability (Damiani et al.,

238   2019). HCP modeling at watershed level could be the best option in this sense. Reach HCPs were

239   thus aggregated according to watershed boundaries defined in the HydroBASINS dataset

240   (Lehner and Grill, 2013) at level 03 and 04 (HB03, HB04), assigning to each river segment the

241   Pfafstetter codes corresponding to the respective watersheds. The formula used for the

242 aggregated characterization factor at watershed (CF_{wt}) was taken from Damiani et al. (2019)

243 where the ratio between individual length of river segments and the total length of all catchment

244 rivers is the weighting factor for HCPs calculated at reach that are subsequently summed up in an

245 aggregated score. However, since high stream order rivers are not included in the European

246 database (Strahler order 1 and part of Strahler order 2), we chose to also aggregate based on

247 average river water volume V (m^3) per month t residing in each river segment, as in Equation 8:

$$CF_{wt} = FF_{wt} \cdot EF_{wt} = \frac{dQ_{wt}}{dCWU_{wt}} \cdot \sum_{i=1}^{n} HCP_{it} \cdot \frac{V_{it}}{\sum_{i=1}^{n} V_{it}} \tag{8}$$

248 where water volume is the product of width W, depth D and length. It was therefore necessary

249 to calculate monthly river depth D, by means of Equation 9, following the same reasoning of

250 Equation 7:

$$D_{it} = \left[c_d \cdot \bar{Q}_i^{f_d} \right] \cdot \left[\frac{Q_{it}}{\bar{Q}_i} \right]^f \tag{9}$$

251 where c_d and f_d are the "downstream" hydraulic geometry parameters for depth, and f is the

252 "at-a-station" exponent (c_d = 0.340, f_d = 0.259, f = 0.292 from the data in Morel et al., 2020). The

253 difference between length and volume weighting is that the first method implies equal weight for

254 all reaches in the drainage basin and missing high order streams would likely bias the result of

255 the characterization. In the latter the quantity of water that a river provides to the drainage basin

256 is the weighting factor. This implies the assumption that the water consumed within a watershed

257 has higher probability of being withdrawn from rivers with higher volume of available water.

258 After aggregation, the outputs of the generalized model were compared to those resulting from

259 the French model to test results consistency. Four watersheds entirely included into French

260 borders were taken into account. *Q90* and August characterization factors were compared for the

261 local and the generalized model respectively. According to the data used for HCP modeling in

262   this study, August is generally the driest month of the year, with exceptions such as in glacier-fed

263   streams. It is therefore more likely to have low flows ($Q90$) occurring in this period of the year.

264   **2.6 Application to European agricultural water use**

265   The global, regionalized HCP model was applied to a case study to discuss its usability and

266   interest for LCA. Agriculture alone is responsible for 70% of global water withdrawals

267   (UNESCO and UN-Water, 2020), 40% in Europe (European Environment Agency, 2018). The

268   impact of 1 m^3 water consumption for agricultural use according to available agricultural water

269   supply mixes was assessed (WSmix, Leão et al., 2018). Calculations were made for selected

270   European countries with agricultural water consumption greater than 1 000 million m^3/year,

271   including Turkey and Azerbaijan (SI, Table S4). Since the HCP model applies to surface water

272   habitats, impact is calculated for the share of surface water in the WSmix. This encompasses

273   generic surface water consumption data, spring water, inter-basin transferred water and

274   reservoirs. Although, artificial impoundments per se are not directly covered by the HCP model

275   which is more sensitive to habitat variation in streams, reservoirs were included because the

276   differentiation between the two types of water sources was available for a few countries only,

277   while in most cases the information is hidden in generic surface water use. Moreover, reservoir

278   water is often used to maintain river flow in dry periods or when water demand is higher, and in

279   this case can thus be considered as stream water, except that abstraction is delayed in time.

280   National annual average HCPs were calculated from watershed HCPs of each country and

281   compared with the AWARE CFs for agriculture at the same spatial and temporal resolution.

282   AWARE quantifies available water remaining after the demand of humans and aquatic

283   ecosystems has been met (Boulay et al., 2018). Since Spain had the best detail on watershed and

284   sub-watershed WSmixes among selected countries in Leão et al. (2018), comparisons between

285   HCP and AWARE were also made at watershed scale for Spanish river basins to discuss spatial

286   scale choices for HCP characterization (SI, Table S5).

287   **3. RESULTS AND DISCUSSION**

288   **3.1 HCP modeling at reach and watershed scale**

289   The mean annual streamflow model applied to European rivers and adjusted with monthly

290   climatic data, allows estimating the seasonal variability in river discharge along the year,

291   deriving from rainfall and temperature. Figure 3 represents the detail of monthly Q and HCP

292   distribution in the selected rivers excluding extreme values (R robustbase package for skewed

293   distributions, Hubert and Vandervieren, 2008). Outliers are not represented because of the size of

294   the data sample and the high variability of European and Middle Eastern climatic conditions and

295   river regimes. The latter would result in extremely low discharge values for small rivers in dry

296   periods (e.g. small streams in the Mediterranean region and the Middle East) and six orders of

297   magnitude greater flows in big rivers during wet months (e.g. in major rivers of continental

298   Europe). For each month, streamflow distribution is right skewed with maximum median and

299   average values of 1.03 m^3/s and 61.58 m^3/s respectively (both in December), reflecting the

300   predominance of small streams in the modeling dataset.

301   A reduction in river discharge in dry months is associated to a lower average Reynolds number

302   in river reaches and therefore to higher habitat change potential for those habitats more likely to

303   be damaged by water deprivation (shallow and well oxygenated running waters). Figure 3

304   confirms the lower availability of water in summer months and the associated higher habitat

305   sensitivity to water consumption. In wet season, indicatively from November to April, 95% of

306   European rivers included in the study fall between discharge values of 0 and 299.6 m^3/s. From

307   May to October Q is between 0 and 37.4 m³/s. The derived HCP is comprised between 0 and

308   4 070.9 m² s/m³ in wet months and between 0 and 13 352.9 m² s/m³ in dry season (see SI, Tables

309   S2 and S3).
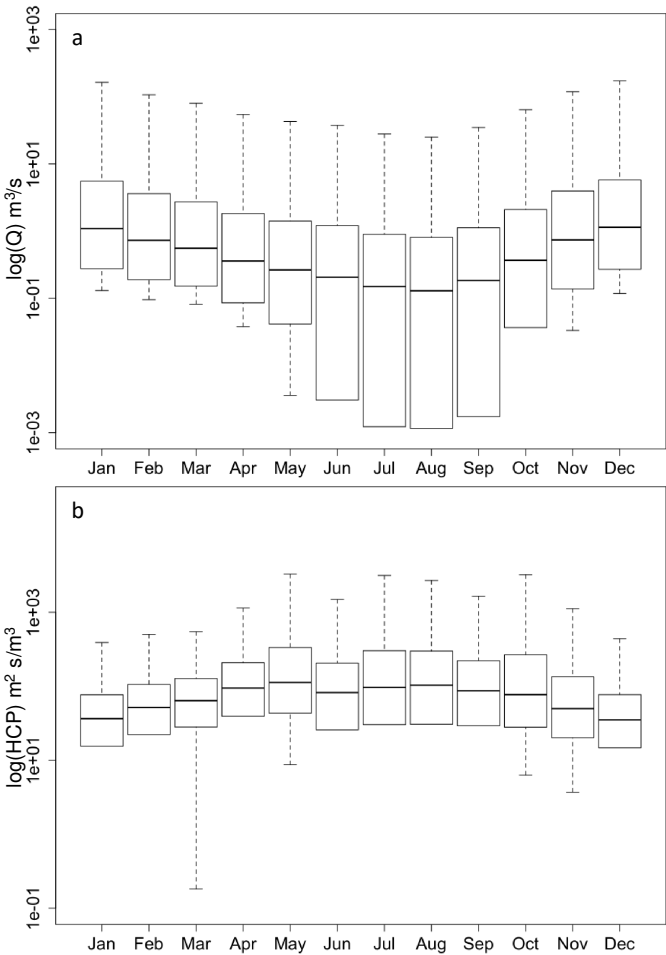
310

311   **Figure 3.** Monthly discharge Q in European rivers (a) and HCP characterization factors

312   distribution (b)

313   Figure 4 illustrates HCP in European and Middle Eastern reaches in January and July.

314   Characterization factors of the other months are shown in SI, Figure S1. The results highlight an

315   increase of habitat change potential in dry season, especially in the Mediterranean region and

316   diffusely in arid areas of the Middle East and the Caspian Sea (Kazakhstan, Turkmenistan, Iran).

317 Dark grey-shaded river segments are those where the HCP model cannot be applied for different

318 reasons. Overall, HCP greater than 25 000 m^2 s/m^3 were considered outside the validity range of

319 the habitat model, according to the scores obtained in the local HCP model (Damiani et al.,

320 2019) from which the generalized model was derived. The maximum amount of such values was

321 observed in August for 44 860 river segments corresponding to 10% of the total. These streams

322 are located essentially in the Middle East and in desert regions, corroborating the non-

323 applicability of the model since it has been developed from river ecosystems pertaining to

324 different climatic regions and hydrological conditions.

325 A characterization factor is also not quantifiable in rivers where discharge is equal to 0.

326 According to the formula used to quantify Q, described in section 2, this may happen for two

327 reasons. The first one is for reaches that are not sustained by runoff fed from rainfall and that

328 cease to flow periodically (Figure 4b). In the modeled dataset this applies to 12.8% of river

329 segments maximum in September, mostly in arid and desert areas. In this case, the global HCP

330 model is not applicable since rivers dry out and no habitat is present. Moreover, it should be

331 considered that the uncertainty deriving from applying the characterization model on non-

332 perennial rivers, such as those represented in Figure 4a and masked out in Figure 4b in the

333 Arabian Peninsula, is high. In Figure 3, the peaks in HCP values in May and October is due to

334 the fact that precipitation and thus a modest value of discharge can be attributed to these rivers at

335 the two boundaries between wet and dry season, resulting in high HCP extremes (SI, Table S3

336 and Figure S1). However, ecosystems of intermittent and ephemeral rivers are still the subject of

337 extensive research (Leigh et al., 2016) and, although potential physical habitat availability can be

338 represented by the HCP indicator, these streams are characterized by specific ecological

339 mechanisms that cannot be exhaustively described by the HCP model.

340 Discharge, and therefore HCP, could not be attributed also in river segments where the altitude

341 is equal to or lower than 0. These conditions are distinctive in estuarine and brackish areas that

342 are out of the scope of the HCP model. Even if fish species are not taken into account, impact of

343 water use on wetland ecosystems is covered by the models proposed by Verones et al. (2013a,

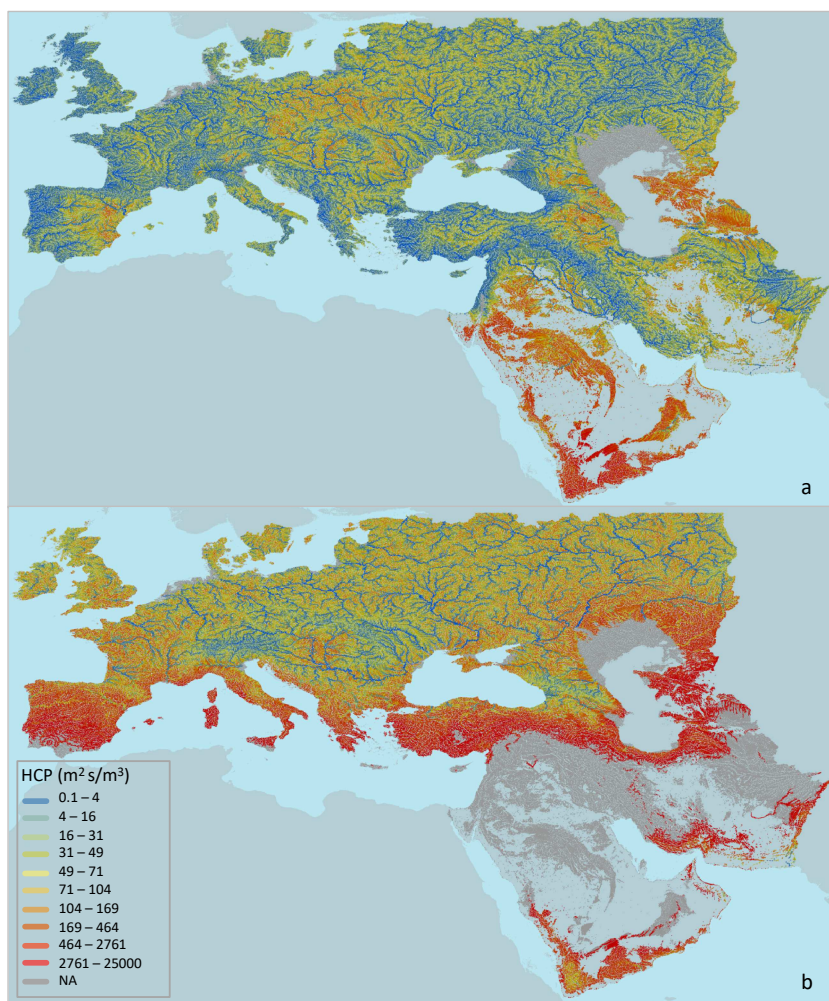344 2013b) which can be therefore complementary to our model.

345

346 **Figure 4.** Habitat change potentials in a) January and b) July

3.2 Watershed characterization factors

Aggregated characterization factors at watershed level reflect the outcomes of reach-scale HCP with higher values during summer months in Mediterranean and arid regions for both aggregation formulas tested on river lengths and volumes (the latter applied in Figure 4). Higher level aggregation at HB03 averages the impact of smaller, contiguous sub-watersheds resulting overall in lower HCP scores. Outcomes of both aggregation methods highlight a decrease of HCP values when volume weighting is performed, as shown in Table 3.
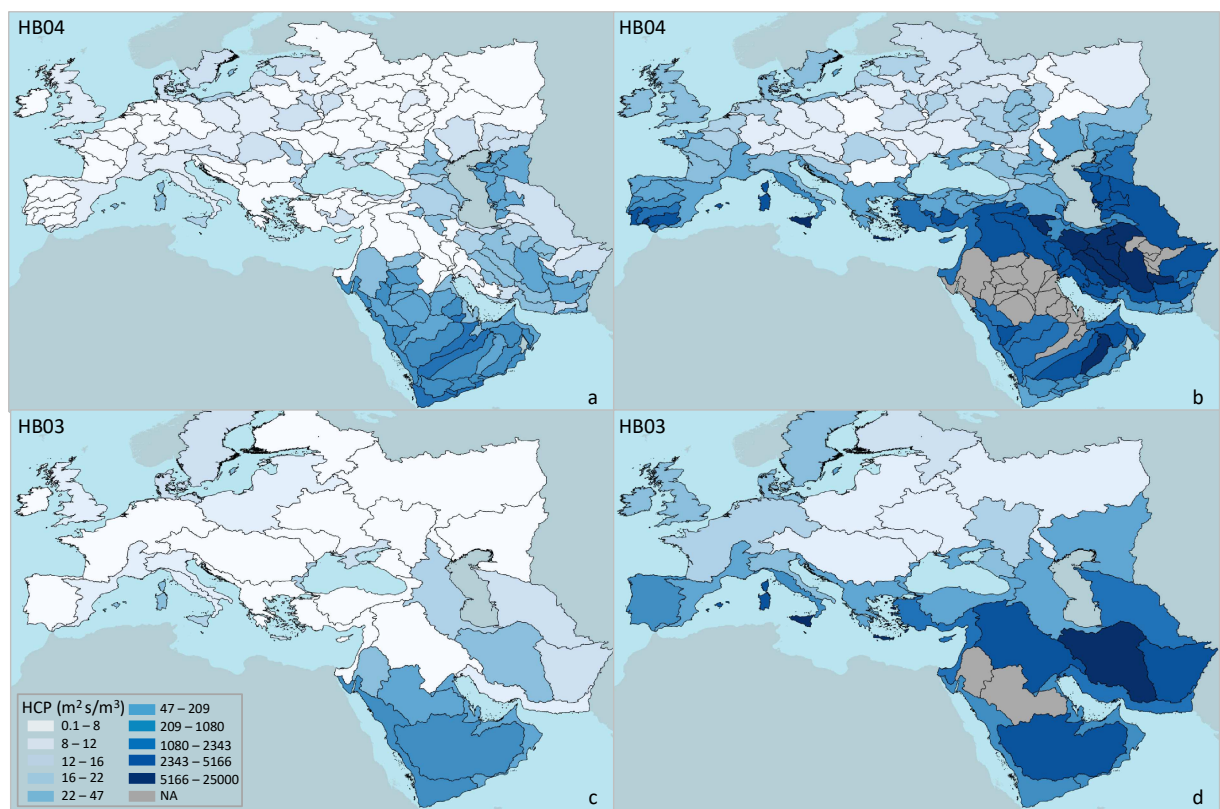

Figure 5. Aggregation of reach-scale HCPs based on water volumes in a) January, HB04; b) July, HB04; c) January, HB03; d) July, HB03

3.3 Consistency analysis

In French watersheds at HB04, the comparison between aggregated HCPs on length in the local model and in the present study showed six times smaller HCP deriving from the generalized model. This is due to the fact that small, high order streams are missing in the European database (Strahler orders 1 and 2 with higher HCP) but not in the detailed French RHT network. Moreover, the relative magnitudes of the characterization value between watersheds are different in both models. Aggregation on volume is therefore preferable as the relationships between watersheds remain consistent and the ratio between local and generalized CFs is decreased to two times when high order streams are taken into account. Recalculating aggregated CFs from the local French model excluding river segments with Strahler order 1 and 2, resulted in further reducing the discrepancy with global HCP scores for France, showing very close characterization factors (Table 3). In absolute terms, these differences are far below the root-mean-squared error associated to the generalized model in equation 4. Uncertainty resulting from deriving a generalized model from a spatially limited one, can be attenuated if at-reach characterization factors are aggregated at watershed scale. Notwithstanding, on a continental scale the deviation of generalized CFs from local CFs is negligible, as demonstrated in Figure 6 for aggregated HCPs.

374 **Table 3.** Comparison between aggregated HCP scores (m^2 s/m^3) for French watersheds from the
375 local model (Q90) and the generalized, global characterization model applied to European river
376 basins (July)

Pfaf	HCP$_l$		HCP$_v$				HCP$_l$ FR/EU	HCP$_v$ FR/EU	HCP$_v$ FR/EU (FR St>1)	HCP$_v$ FR/EU (FR St>2)	FR HCP$_l$/ HCP$_v$	EU HCP$_l$/ HCP$_v$
	FR	EU	FR	FR St>1	FR St>2	EU						
2321	710.2	144.4	65.8	34.0	25.1	33.8	4.9	1.9	1.0	0.7	10.8	4.3
2322	898.8	126.1	72.6	38.6	28.5	26.9	7.1	2.7	1.4	1.1	12.4	4.7
2323	784.4	153.7	109.5	67.0	47.6	73.9	5.1	1.5	0.9	0.6	7.2	2.1
2324	526.6	99.7	44.4	22.4	17.0	18.8	5.3	2.4	1.2	0.9	11.9	5.3
						$\overline{x}$	5.6	2.1	1.1	0.8	10.5	4.1

377 *Pfaf*: Pfafstetter code from HydroBASINS; *St*: Strahler order; *FR*: local French model; *EU*:
378 global model at the European scale; *HCP$_l$*: HCP length *l* weighting; *HCP$_v$*: HCP volume *v*
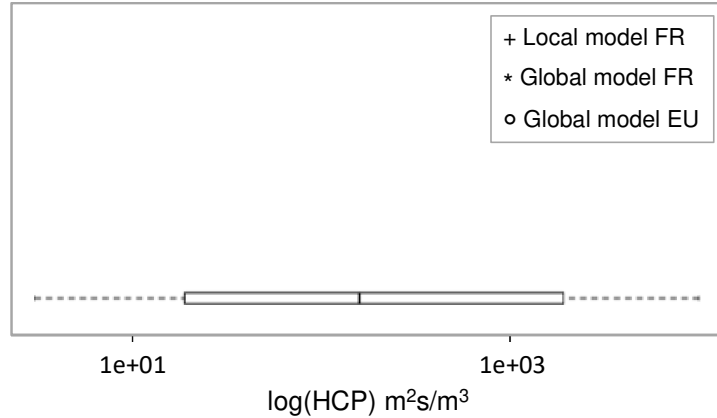379 weighting

380

381 **Figure 6.** Characterization factors for European watersheds with the detail of French watersheds
382 HCP calculated using the generalized (July) and the local model (Q90), including high order
383 streams

3.4 HCP and AWARE for agricultural water use

384

385   When comparing AWARE and HCP it should be kept in mind that indicator units are not the

386   same. While AWARE CFs are dimensionless, the HCP model quantifies the potential alteration

387   in habitat surface (m^2) for marginal discharge change (m^3/s). At country scale, the most evident

388   difference between both characterization approaches depicted in Figure 7a is the country where

389   consuming 1 m^3 of water for agriculture has the greatest impact. AWARE indicates Azerbaijan

390   as the most impacted country, while the highest HCP is attributed to Greece. This is due to

391   intrinsic differences of both models. AWARE represents available water remaining net of water

392   demand by humans and ecosystems (Boulay et al., 2018). As a result, high surface water demand

393   in Azerbaijan (SI, Table S4) is likely to increase the AWARE score compared to countries where

394   human water demand is less intense. On the contrary, HCP indicates habitat sensitivity to water

395   consumption regardless of the use and it is rather dependent on topographical and climatic

396   conditions. CF for Greece appears therefore higher and heavily influenced by HCP of insular

397   areas (e.g. Figure 4 and Figure 5). When the water mix is not taken into account and the impact

398   is allocated on all water sources indifferently, outcomes for Greece are closer in both models (SI,

399   Figure S2). In Ukraine, a relatively large water demand is the main reason for the difference

400   between AWARE and the HCP score, according to which stream habitats appear to be less

401   sensitive to consumptive water use.

402   When corresponding inventory data are available, impact assessment can be brought to

403   watershed level as illustrated in Figure 7b. The same concept discussed above applies to Spanish

404   river basins where the Ebro is the most stressed according to AWARE and the Tinto-Odiel-

405   Piedras catchment shows the highest habitat sensitivity. The HCP value for the Ebro stimulates

406   reflection on the spatial scales used for HCP aggregation. Values for the Ebro, as well as for

407   other sensitive Spanish river basins such as the Jucar or the Segura included in Figure 4, were

408   averaged with reach characterization factors of Southern France at HB04 scale (Figure 5). In

409   critical regions, a narrower spatial resolution could be beneficial to catch the detail of

410   particularly vulnerable watersheds that would otherwise be lost using large scale characterization
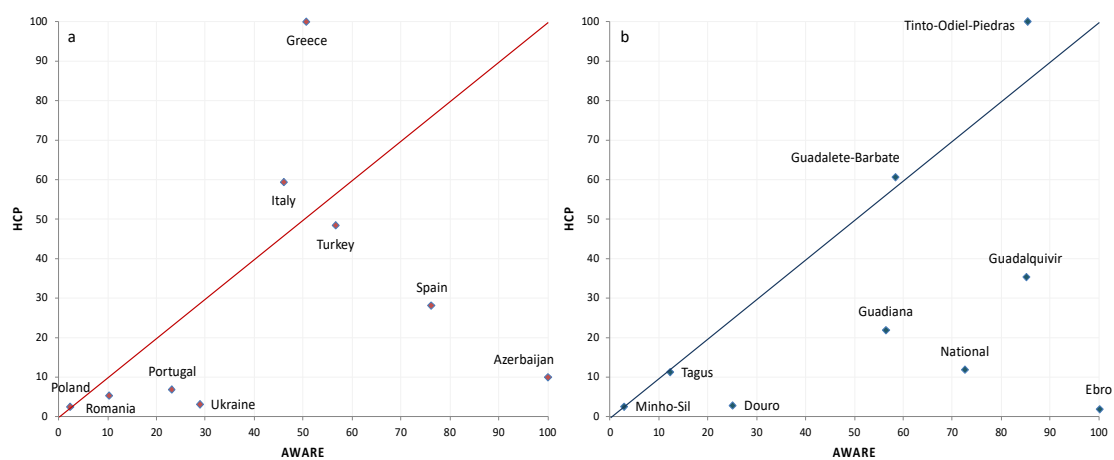
411   factors.

412

413

414   **Figure 7.** Impact of 1 m^3 consumption of surface water for agriculture according to AWARE and

415   HCP characterization models at a) country level and b) watershed scale in Spain

416   **4. CONCLUSIONS AND RESEARCH OUTLOOK**

417   Impact assessment of water consumption through habitat change potential modeling on

418   individual river segments represents an advancement in terms of environmental relevance and

419   spatial resolution of water consumption LCIA models. This study demonstrates the

420   transferability of a high-resolution local HCP model at the continental scale and the validity of

421   the chosen approach. The new model can be used to develop global characterization factors.

422   Results at reach scale highlighted the importance of including small streams in the assessment,

423 since they are the most sensitive to water volume change, and the habitats they harbor are

424 therefore more likely to be affected by consumptive water use.

425   Even if LCA inventories frequently do not support this level of detail, high-resolution

426 characterization could highlight the uncertainty derived from ignoring spatial variability when

427 characterizing at lower spatial resolution. On the other hand, if spatially resolved inventory data

428 are used lower uncertainty could be achieved.

429   In order to facilitate the operationalization of the generalized HCP model, aggregation at

430 watershed has been carried out. However, in regions where HCP at reach is higher, a more

431 refined spatial resolution is preferable. On the contrary, for large watersheds in less vulnerable

432 regions, for instance in Central European river basins, a high level of detail would probably be

433 excessive and counter-productive in terms of inventory data availability. To allow applicability

434 of the HCP model in the short-term, country HCPs can be easily calculated and, even if

435 important details at the watershed scale may be missing, results can be compared with those

436 deriving from existing models such as AWARE. In addition, some interesting differences were

437 highlighted between both models demonstrating the interest of HCP characterization as a

438 complementary indicator focused specifically on assessing impacts on freshwater habitats.

439   The importance of linking inventory data and impact assessment refers as well to the

440 characterization of water consumption from a temporal point of view. For instance, in the

441 example discussed above, annual average CFs were associated to annual WSmix. Monthly CFs

442 are available, but the same detail is not provided by current water consumption data in

443 inventories. Moreover, reservoir water has been included in generic surface water consumption.

444 However, reservoirs can be used to ensure sufficient supply of water volumes needed for human

445 activities and ecosystems in dry season, mitigating water shortage in downstream rivers, which is

446   not taken into account in current models (neither in AWARE nor in the HCP model).

447   Nonetheless, river regulation and inter-basin transfer may involve non-marginal changes in river

448   environmental and ecological conditions that would not be covered by the HCP model as it is.

449   Concerning the temporally resolved assessment of HCP, it should also be considered that the

450   HCP model does not apply to all flow magnitudes. Consequences of a high flow period on

451   freshwater habitats are different than during low flows. Calculating monthly HCP has been

452   necessary because it is not possible to define locally when low and high flows occur. However,

453   monthly discharges used to compute HCP can be still considered averages and therefore high

454   flow peaks are flattened. An alternative to modeling monthly CF would be to derive median

455   and minimum discharge for each river segment as a proxy for *Q50* and *Q90*, and use the resulting

456   HCP for the wet and the dry season respectively, as done in Damiani et al. (2019). This solution

457   could also be compared with HCPs from average and minimum discharge modeled in other

458   existing databases (e.g. Linke et al., 2019). Notwithstanding, the HCP value for high discharge is

459   extremely low and yet likely to be overestimated because deriving from fitting a model on

460   median and low flow HCPs. In addition, given the temporal resolution of HCP being monthly,

461   this is not likely to occur frequently, assuming high flow peaks do not tend to last longer than a

462   couple of weeks. Furthermore, inventory data are currently not likely to reflect temporal

463   resolutions beyond trimestral or seasonal resolution and will in most cases be annual averages.

464   Uncertainty deriving from including potential high flow periods in the characterization is

465   therefore likely to be negligible in practice.

466   It is also important to mention that water consumption LCA could fully take advantage of

467   temporal and spatial quantification of water consumption inventory data and impact

468   characterization, only if inventory and effects are linked by a mechanistic fate factor describing

469 water balance variations in different environmental compartments following withdrawal (e.g.

470 aquifer, river, soil; Núñez et al., 2018).

471   As a long-term perspective, a mechanistic pathway linking water consumption to a fate factor

472 and an effect factor based on HCP allows reach-scale, mechanistic, endpoint impact modeling

473 when combined with information on the biological context at the reach scale. This could include

474 the presence or absence of species or functional guilds adapted to a certain hydraulic habitat

475 (considering also their economic, social, and cultural values). A reduction in river discharge in

476 dry months results in lower average Reynolds number in river reaches and in higher HCP for

477 those habitats, and therefore those species, more vulnerable to water volume alteration.

478 Ecohydrological habitat models at the root of the HCP model are derived from empirical, species

479 abundance data. Relating habitat availability to predicted sensitive species abundance and

480 density, which is currently subject of extensive research (Lamouroux and Olivier, 2015;

481 Mérigoux et al., 2015), could allow developing LCIA indicators of potential abundance when

482 hydraulics is the limiting factor. In addition, regarding hydraulic modeling of river habitat, width

483 and depth equations used in the present study are discharge dependent but can be improved

484 including geomorphological variables, as for instance catchment slopes, geology or landcover

485 (Morel et al., 2020).

486   With the purpose of developing global endpoint models based on freshwater habitat change

487 potential, it is even more crucial to define the range of validity of the model. In the present study,

488 HCP values greater than $25\,000$ m^2 s/m^3 were excluded. These were mostly associated with

489 streams in arid and desert regions that are most likely characterized by ecological conditions

490 different from those on which the HCP model is based. These rivers are predominantly

491 intermittent and identified calculating discharge at monthly resolution. A better, global

492   characterization of intermittent streams from a hydrologic and ecological perspective would

493   certainly improve the applicability of the model in the most arid areas. To limit HCP outliers, the

494   possibility to apply the model on a minimum discharge threshold could also be investigated,

495   based on hydrology, water users, demographics, or water management policies adopted in certain

496   regions.

497   It should also be considered that the generalized model has been developed based on local

498   HCP calculated using habitat preference equations for species that are not ubiquitous. However,

499   it is assumed that hydrological and hydraulic conditions within validity of the HCP model would

500   globally determine the establishment of comparable habitats and the presence (or absence) of

501   species with convergent behavior and habitat preferences (Lamouroux et al., 2002), allowing to

502   define species archetypes to apply the HCP model at the global level for midpoint and endpoint

503   LCIA.

504   **ASSOCIATED CONTENT**

505   A Supporting Information document is available including:

506   •   statistics on modeled streamflow values and HCPs;

507   •   HCP monthly maps;

508   •   data used for the AWARE and HCP model comparison.

516 **REFERENCES**

517 Alcamo, J., Döll, P., Henrichs, T., Kaspar, F., Lehner, B., Rösch, T., Siebert, S., 2003.

518   Development and testing of the WaterGAP 2 global model of water use and availability.

519   Hydrol. Sci. J. 48, 317–337. https://doi.org/10.1623/hysj.48.3.317.45290

520 Andreadis, K.M., Schumann, G.J.P., Pavelsky, T., 2013. A simple global river bankfull width

521   and depth database. Water Resour. Res. 49, 7164–7168. https://doi.org/10.1002/wrcr.20440

522 Barbarossa, V., Huijbregts, M.A.J., Hendriks, A.J., Beusen, A.H.W., Clavreul, J., King, H.,

523   Schipper, A.M., 2017. Developing and testing a global-scale regression model to quantify

524   mean   annual   streamflow.   J.   Hydrol.   544,   479–487.

525   https://doi.org/10.1016/j.jhydrol.2016.11.053

526 Boulay, A.-M., Bare, J., Benini, L., Berger, M., Lathuillière, M., Manzardo, A., Margni, M.,

527   Motoshita, M., Núñez, M., Pastor, A. V., Ridoutt, B., Oki, T., Worbe, S., Pfister, S., 2018.

528   The WULCA consensus characterization model for water scarcity footprints: Assessing

529   impacts of water consumption based on available water remaining (AWARE). Int. J. Life

530   Cycle Assess. 23, 368–378. https://doi.org/10.1007/s11367-017-1333-8

531 Conrad, O., Bechtel, B., Bock, M., Dietrich, H., Fischer, E., Gerlitz, L., Wehberg, J., Wichmann,

532   V., Böhner, J., 2015. System for Automated Geoscientific Analyses (SAGA) v. 2.1.4.

533   Geosci. Model Dev. 8, 1991–2007. https://doi.org/10.5194/gmd-8-1991-2015

534 Dalin, C., Wada, Y., Kastner, T., Puma, M.J., 2017. Groundwater depletion embedded in

535   international food trade. Nature 543, 700–704. https://doi.org/10.1038/nature21403

536   Damiani, M., Lamouroux, N., Pella, H., Roux, P., Loiseau, E., Rosenbaum, R.K., 2019.

537   Spatialized freshwater ecosystem life cycle impact assessment of water consumption based

538   on instream habitat change modeling. Water Res. 163, 1–12.

539   https://doi.org/10.1016/j.watres.2019.114884

540   Damiani, M., Roux, P., Núñez, M., Loiseau, E., Rosenbaum, R.K., 2018. Addressing water needs

541   of freshwater ecosystems in life cycle impact assessment of water consumption : state of the

542   art and applicability of ecohydrological approaches to ecosystem quality characterization.

543   Int. J. Life Cycle Assess. 23, 2071–2088. https://doi.org/https://doi.org/10.1007/s11367-

544   017-1430-8

545   Döll, P., Kaspar, F., Lehner, B., 2003. A global hydrological model for deriving water

546   availability indicators: Model tuning and validation. J. Hydrol. 270, 105–134.

547   https://doi.org/10.1016/S0022-1694(02)00283-4

548   European Environment Agency, 2018. EEA Signals 2018 — Water is life, Eea Signals.

549   Publications Office of the European Union, Copenhagen. https://doi.org/10.2800/52469

550   Fick, S.E., Hijmans, R.J., 2017. WorldClim 2: new 1-km spatial resolution climate surfaces for

551   global land areas. Int. J. Climatol. 37, 4302–4315. https://doi.org/10.1002/joc.5086

552   Hanafiah, M.M., Xenopoulos, M. a, Pfister, S., Leuven, R.S.E.W., Huijbregts, M. a J., 2011.

553   Characterization factors for water consumption and greenhouse gas emission based on

554   freshwater fish species extinction. Environ. Sci. Technol. 45, 5272–5278.

555   Hubert, M., Vandervieren, E., 2008. An adjusted boxplot for skewed distributions. Comput. Stat.

556   Data Anal. 52, 5186–5201. https://doi.org/10.1016/j.csda.2007.11.008

557   Janse, J.H., Kuiper, J.J., Weijters, M.J., Westerbeek, E.P., Jeuken, M.H.J.L., Bakkenes, M.,

558   Alkemade, R., Mooij, W.M., Verhoeven, J.T.A., 2015. GLOBIO-Aquatic, a global model of

559   human impact on the biodiversity of inland aquatic ecosystems. Environ. Sci. Policy 48,

560   99–114. https://doi.org/10.1016/j.envsci.2014.12.007

561   Lamouroux, N., Capra, H., 2002. Simple predictions of instream habitat model outputs for target

562   fish   populations.   Freshw.   Biol.   47,   1543–1556.   https://doi.org/10.1046/j.1365-

563   2427.2002.00879.x

564   Lamouroux, N., Olivier, J.M., 2015. Testing predictions of changes in fish abundance and

565   community structure after flow restoration in four reaches of a large river (French Rhône).

566   Freshw. Biol. 60, 1118–1130. https://doi.org/10.1111/fwb.12324

567   Lamouroux, N., Poff, N.L., Angermeier, P.L., 2002. Intercontinental Convergence of Stream

568   Fish Community Traits Along Geomorphic and Hydraulic Gradients. Ecology 83, 1792–

569   1807. https://doi.org/10.1890/0012-9658(2002)083[1792:ICOSFC]2.0.CO;2

570   Lamouroux, N., Souchon, Y., 2002. Simple predictions of instream habitat model outputs for fish

571   habitat guilds in large streams. Freshw. Biol. 47, 1531–1542. https://doi.org/10.1046/j.1365-

572   2427.2002.00879.x

573   Leão, S., Roux, P., Núñez, M., Loiseau, E., Junqua, G., Sferratore, A., Penru, Y., Rosenbaum,

574   R.K., 2018. A worldwide-regionalised water supply mix (WSmix) for life cycle inventory

575   of   water   use.   J.   Clean.   Prod.   172,   302–313.

576   https://doi.org/https://doi.org/10.1016/j.jclepro.2017.10.135

577   Lehner, B., Grill, G., 2013. Global river hydrography and network routing: baseline data and

578   new approaches to study the world's large river systems. Hydrol. Process. 27, 2171–2186.

579   https://doi.org/10.1002/hyp.9740

580   Leigh, C., Boulton, A.J., Courtwright, J.L., Fritz, K., May, C.L., Walker, R.H., Datry, T., 2016.

581   Ecological research and management of intermittent rivers: an historical review and future

582   directions. Freshw. Biol. 61, 1181–1199. https://doi.org/10.1111/fwb.12646

583   Leopold, L.B., Maddock, T., 1953. The Hydraulic Geometry of Stream Channels and Some

584   Physiographic Implications, Geological Survey Professional Paper 252. Washington, DC.

585   Linke, S., Lehner, B., Dallaire, C.O., Ariwi, J., Grill, G., Anand, M., Beames, P., Burchard-

586   levine, V., Moidu, H., Tan, F., Thieme, M., 2019. HydroATLAS : global hydro-

587   environmental sub-basin and river reach characteristics at high spatial resolution 0–25.

588   https://doi.org/10.1038/s41597-019-0300-6

589   Loiseau, E., Aissani, L., Le Féon, S., Laurent, F., Cerceau, J., Sala, S., Roux, P., 2018. Territorial

590   Life Cycle Assessment (LCA): What exactly is it about? A proposal towards using a

591   common terminology and a research agenda. J. Clean. Prod. 176, 474–485.

592   https://doi.org/10.1016/j.jclepro.2017.12.169

593   Mérigoux, S., Forcellini, M., Dessaix, J., Fruget, J.F., Lamouroux, N., Statzner, B., 2015. Testing

594   predictions of changes in benthic invertebrate abundance and community structure after

595   flow restoration in a large river (French Rhône). Freshw. Biol. 60, 1104–1117.

596   https://doi.org/10.1111/fwb.12422

597   Moran, D., Kanemoto, K., 2017. Identifying the Species Threat Hotspots from Global Supply

598   Chains. Nat. Ecol. Evol. 1, 1–5. https://doi.org/doi:10.1038/s41559-016-0023

599   Morel, M., Booker, D.J., Gob, F., Lamouroux, N., 2020. Intercontinental predictions of river

600   hydraulic geometry from catchment physical characteristics. J. Hydrol. 582, 124292.

601   https://doi.org/10.1016/j.jhydrol.2019.124292

602   Nitschelm, L., Aubin, J., Corson, M.S., Viaud, V., Walter, C., 2016. Spatial differentiation in

603   Life Cycle Assessment LCA applied to an agricultural territory: Current practices and

604   method development. J. Clean. Prod. 112, 2472–2484.

605   https://doi.org/10.1016/j.jclepro.2015.09.138

606   Núñez, M., Bouchard, C.R., Bulle, C., Boulay, A.M., Margni, M., 2016. Critical analysis of life

607   cycle impact assessment methods addressing consequences of freshwater use on ecosystems

608   and recommendations for future method development. Int. J. Life Cycle Assess. 21, 1799–

609   1815. https://doi.org/10.1007/s11367-016-1127-4

610   Núñez, M., Rosenbaum, R.K., Karimpour, S., Boulay, A.-M., Lathuillière, M.J., Margni, M.,

611   Scherer, L., Verones, F., Pfister, S., 2018. A multimedia hydrological fate modelling

612   framework to assess water consumption impacts in Life Cycle Assessment. Environ. Sci.

613   Technol. 52, 4658–4667. https://doi.org/10.1021/acs.est.7b05207

614   Palmer, M.A., Lettenmaier, D.P., Poff, N.L., Postel, S.L., Richter, B., Warner, R., 2009. Climate

615   change and river ecosystems: Protection and adaptation options. Environ. Manage. 44,

616   1053–1068. https://doi.org/10.1007/s00267-009-9329-1

617   Park, C.C., 1977. World-wide variations in hydraulic geometry exponents of stream channels: an

618   analysis and some observations. J. Hydrol. 33, 133–146. https://doi.org/10.1016/0022-

619 1694(77)90103-2

620 Pastor, A. V., Ludwig, F., Biemans, H., Hoff, H., Kabat, P., 2014. Accounting for environmental

621   flow requirements in global water assessments. Hydrol. Earth Syst. Sci. 18, 5041–5059.

622   https://doi.org/10.5194/hess-18-5041-2014

623 Pekel, J., Cottam, A., Gorelick, N., Belward, A.S., 2016. High-resolution mapping of global

624   surface water and its long-term changes. Nature 540, 418–422.

625   https://doi.org/10.1038/nature20584

626 Pella, H., Lejot, J., Lamouroux, N., Snelder, T., 2012. Le réseau hydrographique théorique

627   (RHT) français et ses attributs environnementaux. Géomorphologie Reli. Process. Environ.

628   18, 317–336. https://doi.org/10.4000/geomorphologie.9933

629 Pfister, S., Koehler, A., Hellweg, S., 2009. Assessing the environmental impacts of freshwater

630   consumption in LCA. Environ. Sci. Technol. 43, 4098–4104.

631   https://doi.org/10.1021/es802423e

632 Quantum GIS Development Team, 2017. Quantum GIS Geographic Information System.

633 R Core Team, 2016. R: A language and environment for statistical computing.

634 Rhodes, D.D., 1978. World-wide variations in hydraulic geometry exponents of stream channels:

635   an analysis and some observations — comments 39, 193–197. https://doi.org/10.1016/0022-

636   1694(78)90123-3

637 RStudio Team, 2016. RStudio: integrated development environment for R.

638 Tendall, D.M., Hellweg, S., Pfister, S., Huijbregts, M. a J., Gaillard, G., 2014. Impacts of river

639   water consumption on aquatic biodiversity in life cycle assessment - a proposed method,

640   and a case study for Europe. Environ. Sci. Technol. 48, 3236–44.

641   https://doi.org/10.1021/es4048686

642   UNESCO, UN-Water, 2020. The United Nations World Water Development Report 2020: Water

643   and Climate Change. Paris.

644   Verones, F., Pfister, S., Hellweg, S., 2013a. Quantifying area changes of internationally

645   important wetlands due to water consumption in LCA. Environ. Sci. Technol. 47, 9799–

646   9807. https://doi.org/10.1021/es400266v

647   Verones, F., Pfister, S., van Zelm, R., Hellweg, S., 2017. Biodiversity impacts from water

648   consumption on a global scale for use in life cycle assessment. Int. J. Life Cycle Assess. 22,

649   1247–1256. https://doi.org/10.1007/s11367-016-1236-0

650   Verones, F., Saner, D., Pfister, S., Baisero, D., Rondinini, C., Hellweg, S., 2013b. Effects of

651   consumptive water use on biodiversity in wetlands of international importance. Environ.

652   Sci. Technol. 47, 12248–12257. https://doi.org/10.1021/es403635j

653   Vörösmarty, C.J., McIntyre, P.B., Gessner, M.O., Dudgeon, D., Prusevich, A., Green, P.,

654   Glidden, S., Bunn, S.E., Sullivan, C.A., Liermann, C.R., Davies, P.M., 2010. Global threats

655   to human water security and river biodiversity. Nature 467, 555–561.

656   https://doi.org/doi:10.1038/nature09440

657   Vörösmarty, C.J., Pahl-Wostl, C., Bunn, S.E., Lawford, R., 2013. Global water, the anthropocene

658   and the transformation of a science. Curr. Opin. Environ. Sustain. 5, 539–550.

659   https://doi.org/10.1016/j.cosust.2013.10.005